Weierstraß-Institut
für Angewandte Analysis und Stochastik
Leibniz-Institut im Forschungsverbund Berlin e. V.

Preprint ISSN 2198-5855

Reliable averaging for the primal variable in the Courant FEM and hierarchical error estimators on red-refined meshes

Carsten Carstensen[1], Martin Eigel[2]

submitted: April 22, 2016

[1] Humboldt-Universität zu Berlin
Unter den Linden 6
10099 Berlin
Germany
E-Mail: cc@mathematik.hu-berlin.de

[2] Weierstrass Institute
Mohrenstr. 39
10117 Berlin
Germany
E-Mail: martin.eigel@wias-berlin.de

No. 2251
Berlin 2016

2010 *Mathematics Subject Classification.* 35J15, 46E22, 49Q10, 49K20, 49K40.

Key words and phrases. A posteriori, error analysis, finite element method, averaging, smoothing,hierarchical estimator, adaptivity, mesh refinement, convergence.

Research of the second author was funded in part by the DFG MATHEON project C33. Part of the work was carried out during a research stay supported by the World Class University (WCU) program through the National Research Foundation of Korea (NRF) funded by the Ministry of Education, Science and Technology R31-2008-000-10049-0.

Edited by
Weierstraß-Institut für Angewandte Analysis und Stochastik (WIAS)
Leibniz-Institut im Forschungsverbund Berlin e. V.
Mohrenstraße 39
10117 Berlin
Germany

Fax: +49 30 20372-303
E-Mail: preprint@wias-berlin.de
World Wide Web: http://www.wias-berlin.de/

Abstract

A hierarchical a posteriori error estimator for the first-order finite element method (FEM) on a red-refined triangular mesh is presented for the 2D Poisson model problem. Reliability and efficiency with some explicit constant is proved for triangulations with inner angles smaller than or equal to $\pi/2$. The error estimator does not rely on any saturation assumption and is valid even in the pre-asymptotic regime on arbitrarily coarse meshes. The evaluation of the estimator is a simple post-processing of the piecewise linear FEM without any extra solve plus a higher-order approximation term. The results also allows the striking observation that arbitrary local averaging of the primal variable leads to a reliable and efficient error estimation. Several numerical experiments illustrate the performance of the proposed a posteriori error estimator for computational benchmarks.

1 Introduction

1.1 Averaging of the dual variable

Averaging techniques are extremely popular in finite element applications because of their obvious simplicity and universality as well as their observed amazingly high accuracy in many numerical simulations [ZZ87]. Their theoretical foundation is less obvious and, in many applications, the use of averaging schemes remains indeed doubtful; see [Car04, CBK01, CB02, BC02, CF01] for positive results. The simplest setting for an explanation of dual and primal variables and their averaging is the 2D Poisson problem with given right-hand side $f \in L^2(\Omega)$ in a polygonal Lipschitz domain Ω and a unique weak solution $u \in H^1_0(\Omega)$ to

$$-\Delta u = f \quad \text{in } \Omega \quad \text{and} \quad u = 0 \quad \text{on } \partial\Omega. \tag{1.1}$$

The primal variable u (displacement or velocity, etc.) and the dual variable $p := \nabla u$ (flux or stress, etc.) are approximated by a finite element solution $u_h \in V_1(\mathcal{T}) := P_1(\mathcal{T}) \cap H^1_0(\Omega)$ with

$$a(u_h, v_h) = F(v_h) \quad (v_h \in V_1(\mathcal{T})).$$

Here, $P_1(\mathcal{T})$ denotes the piecewise affine functions with respect to a triangulation $\mathcal{T}$ and $H^1_0(\Omega)$ is the standard Sobolev space (cf. Section 1.7 below for more details). In fact, u (resp. u_h) is the Riesz representation of the functional $F \in H^{-1}(\Omega)$ defined by $F(v) := \int_\Omega fv\ dx$ (resp. $F|_{V_1(\mathcal{T})} \in V_1(\mathcal{T})^*$) in the Hilbert space $(H^1_0(\Omega), a)$ (resp. $(V_1(\mathcal{T}), a|_{V_1(\mathcal{T})\times V_1(\mathcal{T})})$) with energy scalar product

$$a(v, w) := \int_\Omega \nabla v \cdot \nabla w\ dx \qquad \big(v, w \in H^1_0(\Omega)\big)$$

and induced energy norm $|||\bullet||| := a(\bullet, \bullet)^{1/2}$.

The justification of dual averaging (namely flux or stress averaging) was in dispute between engineers and mathematicians for a long time until it became clear that *all averaging is reliable* in the sense that

$$|||u - u_h||| \leq c_1 \min_{q_h \in Q(\mathcal{T})} \|p_h - q_h\| + c_2 \operatorname{osc}(f, \mathcal{N})$$

for any piecewise polynomial subspace $Q(\mathcal{T})$ of $H(\operatorname{div}, \Omega)$. The discrete flux $p_h := \nabla u_h$ is approximated by any post-processed q_h with respect to the L^2 norm $\|\bullet\| := \|\bullet\|_{L^2(\Omega)}$ and $\operatorname{osc}(f, \mathcal{N})$ denotes node-oriented higher-order data oscillations. The constants c_1 and c_2 depend on the interior angles in $\mathcal{T}$ and the polynomial degree $\leq k$ of

$$Q(\mathcal{T}) \subseteq P_k(\mathcal{T})^2 \cap H(\operatorname{div}, \Omega)$$

but are independent of u, f or any mesh-size in $\mathcal{T}$. The reliability proof goes back essentially to the dominance of the edge contributions in standard residual-based error control by [Rod94] and can be found in [Car99, CV99] for the Poisson problem at hand and in [CB02, CF01] for related problems.

1.2 Averaging of the primal variable

The situation is less clear for primal averaging where the primal variable u_h is post-processed by some $v_h \in H_0^1(\mathcal{T})$. The standard justification is based on some super-closeness result

$$|||u - v_h||| \leq c_3 \, |||u_h - v_h||| \tag{1.2}$$

for some known $v_h \in H_0^1(\Omega)$ and $0 < c_3 < \infty$. A triangle inequality shows

$$|||u - u_h||| \leq |||u - v_h||| + |||v_h - u_h||| \leq (1 + c_3) \, |||u_h - v_h|||$$

and therefore leads to reliability of the computable term $|||u_h - v_h|||$. The main difficulty is the proof of (1.2) for the post-processed approximation v_h. Super-convergence results are employed to justify (1.2) or even some estimate

$$|||u - v_h||| \leq q \, |||u - u_h||| \quad \text{for some } 0 < q < 1. \tag{1.3}$$

In this case, a triangle inequality leads to

$$|||u - u_h||| \leq |||u - v_h||| + |||u_h - v_h||| \leq q \, |||u - u_h||| + |||u_h - v_h|||$$

and hence leads to reliability of the error estimator $|||u_h - v_h|||$ in the sense of

$$|||u - u_h||| \leq (1 - q)^{-1} \, |||u_h - v_h||| \, .$$

We refer to [CGG15, DN02, Noc93, Ago02] for some positive results of the type (1.3) up to perturbations in form of oscillations or higher-order approximation terms. Those results play an important rôle in the dual weighted residual method [BR03, BR01] as well as in the hierarchical error control [BS93, BW85, AO00, BEK96, AAA04]. The first main difficulty is the trade-off of computational costs versus accuracy: If v_h denotes a higher-order approximation (e.g. a quadratic

FEM approximation [DN02]) or an approximation of a red-refined mesh $\mathrm{red}(\mathcal{T})$ [Noc93, CGG15], positive results are known which even lead to convergent adaptive algorithms like [FLOP10]. However, the computation of v_h may appear to be too costly. The second difficulty is the fact that super-convergence (1.3) requires higher smoothness of the exact solution u and may even be observed solely in the asymptotic regime for very fine meshes. It usually remains unclear whether a given triangulation $\mathcal{T}$ (e.g. $\mathcal{T}_H$ from Figure 1) is sufficiently fine or how the constant q or c_3 can be computed for the mesh $\mathcal{T}$ at hand.

1.3 New hierarchical error estimator

Given a triangulation $\mathcal{T}_H$ and its red-refinement $\mathcal{T}_h$ with P_1 conforming FE solution u_h and P_2 interpolation $I_2 u_h$ on $\mathcal{T}_H$, the estimator $\eta_h := |||u_h - I_2 u_h|||$ is a reliable error estimator in the sense that

$$|||u - u_h||| \leq 4/\sqrt{7}(\eta_h + |||u - u_H|||),$$

where u_H is a P_2 best approximation to u. This follows from Theorem 2.2 below. The higher-order term can be controlled by

$$|||u - u_H||| \leq C_1(\eta_h + \mathrm{osc}(f, \{\omega_z \mid z \in \mathcal{N}\}))$$

with some generic constant C_1 and patch-oriented oscillations of the right-hand side f as proven in Corollary 3.7 below.

The hierarchical error estimator also justifies some refinement of [CV99] in the sense that the error $|||u - u_h|||$ is controlled by the edge-contributions $[\partial u_h/\partial \nu_F]$ over all edges F in $\mathcal{T}_h$ which do *not* belong to the skeleton of $\mathcal{T}_H$ plus patch-oriented oscillation terms.

1.4 Example for coarse mesh

A simple example for the Poisson model problem with right-hand side $f = 1$ shall motivate and illustrate the limitations of the error analysis carried out in this paper. The square domain is divided into two triangles which form the triangulation $\mathcal{T}_H := \{T_1, T_2\}$ of Figure 1. The discrete solution $u_h \in P_1(\mathcal{T}_h)$ is evaluated on the uniform red-refined mesh $\mathcal{T}_h = \mathrm{red}(\mathcal{T}_H)$. The error estimator η_h defined above is a simple postprocessing into piecewise quadratic polynomials on the coarse mesh and does not require any global solve. Theorem 2.2 implies $|||u - u_h||| \leq 4/\sqrt{7}\eta_h + \text{h.o.t.}$ despite the fact that u_h and $u_H := I_2 u_h$ both feature just a single degree of freedom (α_5 of Figure 1). By Corollary 3.7, the higher-order term h.o.t. $\leq C_1 \eta_h$ with an unknown constant C_1 which depends only on the interior angles of $\mathcal{T}_H$. In other words, $|||u - u_h||| \leq (4/\sqrt{7} + C_1)\eta_h$ is a guaranteed upper bound even for the coarse mesh of Figure 1. A simple calculation in Subsection 4.1 yields

$$|||u - u_h||| \leq 4/\sqrt{7}\alpha_5 + \text{h.o.t.} = 0.0945 + \text{h.o.t.}$$

Compared to a reference solution u_{ref} evaluated on a fine mesh, the error estimator overestimates the error $|||u_{\text{ref}} - u_h||| = 1/16$ by the factor $3/2$ if the higher-order term were negligible. However, since here h.o.t. $= 0.0452$, it initially has the same order as the error estimator $\eta_h = 0.0650$ and leads to an even larger overestimation.

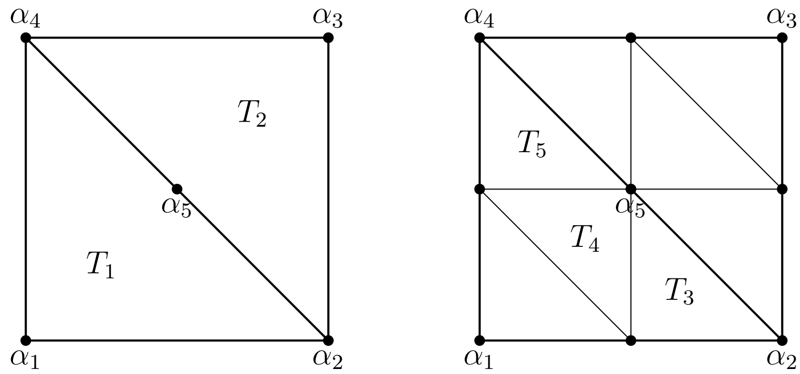

Figure 1: Simplest triangulation $\mathcal{T}_H$ of a square domain with single degree of freedom α_5 for the quadratic interpolant $I_2 u_h \in P_2(\mathcal{T}_H)$ [left] and red-refined triangulation for the evaluation of the discrete solution $u_h \in P_1(\mathrm{red}(\mathcal{T}_H))$ [right].

1.5 Main results

This paper contributes to the important questions discussed above and leads to the following new results.

(a) The design and analysis of an averaging a posteriori error estimator for the primal variable based on the approximation of u on two function spaces of different approximation order.

(b) An interesting observation that the inner jumps on a patch induce a norm equivalent to the error estimator and thus equivalent to the error. This refines [CV99] for red-refined meshes.

(c) The striking general result that *any* local averaging is reliable even pre-asymptotically. This complements the results in [CV99, CB02, BC02] and [FLOP10].

1.6 Outline

The remaining parts of this paper are structured as follows. In the next section, the Poisson model problem and the employed function spaces are introduced in some detail. We recall and extend the framework of [CP07] before we define and analyse an hierarchical a posteriori error estimator which is reliable and efficient asymptotically. By the reduction to a finite-dimensional generalised eigenvalue problem, an explicit upper bound for the error is determined in Section 2. Section 3 examines the interesting equivalence of the error estimator and the jumps of the solution on inner edges on each red-refined triangles. Subsection 3.3 establishes that *all local averaging is reliable*. Numerical examples in Section 4 demonstrate the accuracy of the a posteriori error estimator of Section 2 with efficiency indices in the range of 2 to 4.

1.7 Basic notation

Throughout this paper, the standard notation for Lebesgue and Sobolev spaces is utilized [Bra07, BS08]. In particular, $H^1(\Omega)$ is the Sobolev space of L^2-functions with square integrable first order derivatives on Ω and $H^{1/2}(\partial\Omega)$ denotes the corresponding trace space; ∇ is the gradient and D^2 is the Hessian. We assume $\Omega \subset \mathbb{R}^2$ to be a Lipschitz domain with polygonal boundary $\partial\Omega$ partitioned by a regular triangulation $\mathcal{T}$ into triangles. Any pairwise intersection of distinct triangles is either empty, a vertex in the node set $\mathcal{N}$, or an edge in the edge set $\mathcal{E}$. Subsets of $\mathcal{E}$ are the boundary edges $\mathcal{E}(\partial\Omega) := \{E \in \mathcal{E} \mid E \subseteq \partial\Omega\}$ and the interior edges $\mathcal{E}(\Omega) := \mathcal{E} \setminus \mathcal{E}(\partial\Omega)$. The vector space of polynomials of maximal degree $k \in \mathbb{N}_0$ on a triangle T is denoted $P_k(T)$ and, correspondingly,

$$P_k(\mathcal{T}) := \{v \in L^\infty(\Omega) \mid \forall T \in \mathcal{T}\ v|_T \in P_k(T)\}$$

for the triangulation $\mathcal{T}$. For two adjacent triangles $T_+, T_- \in \mathcal{T}$ with $E \in \mathcal{E}$, $E = T_+ \cap T_-$ and uniquely defined normal vector ν_E on E, the jump of a function $v \in H^1(\Omega)^2$ over $E \in \mathcal{E}$ is denoted by $[v]_E := v|_{T_+} - v|_{T_-}$, where $\nu_E = \nu_{T_+}|_E = -\nu_{T_-}|_E$. The restriction of a function onto some edge is to be understood in the sense of traces. We define the diameter of some $T \in \mathcal{T}$ (resp. $E \in \mathcal{E}$) by $h_T := \operatorname{diam}(T)$ (resp. $h_E := \operatorname{diam}(E)$) and its area by $|T|$ (resp. length $|E| = h_E$). Additionally, let the piecewise constant functions $h_\mathcal{T} : \Omega \to P_0(\mathcal{T})$ and $h_\mathcal{E} : \Omega \to P_0(\mathcal{E})$ be such that, for any $T \in \mathcal{T}$ and $E \in \mathcal{E}$, $h_\mathcal{T}|_T = h_T$ and $h_\mathcal{E}|_E = h_E$.

The red-refinement $\operatorname{red}(T)$ of a triangle T results in a partition into four congruent sub-triangles by connecting the edge mid-points $\operatorname{mid}(\mathcal{E}(T))$ by three new edges.

On some triangle $T \in \mathcal{T}$, we define the integral mean of $f \in L^2(\Omega)$ by $f_T := \int_T f\ dx / |T|$ and the oscillation by

$$\operatorname{osc}(f, T) := h_T \|f - f_T\|_{L^2(T)} \text{ and } \operatorname{osc}(f, \mathcal{T}) := \left(\sum_{T \in \mathcal{T}} \operatorname{osc}^2(f, T)\right)^{1/2}.$$

Given any $z \in \mathcal{N}$, let

$$\mathcal{T}(z) := \{T \in \mathcal{T} \mid z \in T\} \quad \text{and} \quad \mathcal{E}(z) := \{E \in \mathcal{E} \mid z \in E\}.$$

The patch of z is given by $\omega_z := \operatorname{int}\left(\cup\{T \in \mathcal{T} \mid z \in T\}\right)$. Oscillations subject to patches are defined in the same way as before and denoted by $\operatorname{osc}(f, \mathcal{N}) := (\sum_{z \in \mathcal{N}(\Omega)} \operatorname{osc}^2(f, \omega_z))^{1/2}$.

To avoid unnecessary miscellaneous constants, we employ the notation $a \lesssim b$ and $a \approx b$ to denote $a \leq Cb$ and $b \lesssim a \lesssim b$ with generic constant C which only depends on lower bounds of interior angles of triangles in $\mathcal{T}$.

2 Primal Averaging on Large and Small Patches

We consider the Poisson model problem on the open bounded Lipschitz domain $\Omega \subset \mathbb{R}^2$ with polygonal boundary $\partial\Omega =: \Gamma$. Moreover, $u_D \in C(\Gamma) \cap H^2(\mathcal{E}(\Gamma)) = \{w \in C(\Gamma) \mid \forall E \in$

$\mathcal{E}(\Gamma), w|_E \in H^2(E)\}$ is the inhomogeneous Dirichlet data extended to a (e.g. harmonic) function $u_D \in H^1(\Omega)$. The exterior unit normal along the boundary is denoted by ν. With source $f \in L^2(\Omega)$, the model problem reads

$$\begin{aligned} -\Delta u &= f && \text{in } \Omega, \\ u &= u_D && \text{on } \Gamma. \end{aligned} \tag{2.1}$$

We introduce two finite-dimensional spaces used in our error estimator. Let $\mathcal{T}_H$ be a regular triangulation of $\Omega \subset \mathbb{R}^2$ with its set of nodes $\mathcal{N}_H$ and the uniform red refinement $\mathcal{T}_h := \mathrm{red}(\mathcal{T}_H)$ with its set of nodes $\mathcal{N}_h$, $k \in \mathbb{N}$. The corresponding test spaces read

$$V_1 := P_1(\mathcal{T}_h) \cap C_D(\overline{\Omega}) \quad \text{and} \quad V_2 := P_2(\mathcal{T}_H) \cap C_D(\overline{\Omega}), \tag{2.2}$$

where $C_D(\overline{\Omega}) := \{v \in C(\overline{\Omega}) \mid v|_\Gamma = 0\}$. We make use of the nodal interpolation operators

$$I_1 : C(\overline{\Omega}) \to P_1(\mathcal{T}_h) \cap C(\overline{\Omega}) \quad \text{and} \quad I_2 : C(\overline{\Omega}) \to P_2(\mathcal{T}_H) \cap C(\overline{\Omega}).$$

Note that the standard definition of I_2 in $P_2(\mathcal{T}_H)$ uses the nodes of $\mathcal{T}_h$ and so $I_2 I_1 = I_2$. Since for an arbitrary continuous Dirichlet boundary function u_D, the approximation on the boundary is not exact, we introduce $u_{\mathrm{DH}} \in P_2(\mathcal{T}_H) \cap C(\overline{\Omega})$ and $u_{\mathrm{Dh}} \in P_1(\mathcal{T}_h) \cap C(\overline{\Omega})$ as some suitable approximations to u_D when restricted on Γ [BCD04].

Throughout this paper we assume that the following compatibility condition for the Dirichlet data on the spaces V_1 and V_2 is satisfied,

$$\begin{aligned} u_{\mathrm{Dh}} &= I_1 u_D \in P_1(\mathcal{T}_h) \cap C(\overline{\Omega}), \\ u_{\mathrm{DH}} &= I_2 u_{\mathrm{Dh}} = I_2 u_D \in P_2(\mathcal{T}_H) \cap C(\overline{\Omega}). \end{aligned}$$

The weak formulation seeks $u \in H^1(\Omega)$ with the condition $u|_\Gamma = u_D$ on the Dirichlet boundary Γ (in the sense of traces) such that

$$a(u, v) = \int_\Omega f v \, dx \ \text{ for all } v \in V := \{v \in H^1(\Omega) \mid v|_\Gamma = 0\}.$$

Given a bounded linear form $F \in V^*,\ F(v) := \int_\Omega f v \, dx$, and $u - u_D \in V$, the weak solution satisfies $u \in u_D + V$ and

$$a(u, v) = F(v) \qquad \text{for all } v \in V.$$

The goal is an estimate of the unknown error

$$e := u - u_h$$

for the discrete solution $u_h \in u_{\mathrm{Dh}} + V_1$ to

$$a(u_h, v_h) = F(v) \qquad \text{for all } v_h \in V_1. \tag{2.3}$$

In [CP07], the error estimator

$$\eta := \min_{v_H \in u_{\mathrm{DH}} + V_2} \left\| u_h - v_H \right\| \tag{2.4}$$

was shown to be reliable for parameter k sufficiently large. The proof relies on the approximation assumption

$$\delta_{hH} := \frac{\min_{v_H \in u_{\mathrm{DH}} + V_2} \left\| u - v_H \right\|}{\min_{v_h \in u_{\mathrm{Dh}} + V_1} \left\| u - v_h \right\|} = O(1) \tag{AA}$$

and the discrete property

$$q := \max_{v_H \in V_2 \setminus \{0\}} \min_{v_h \in V_1} \frac{\left\| v_H - v_h \right\|}{\left\| v_H \right\|} < 1. \tag{DP}$$

The following theorem is an extension of the main result of [CP07] to inhomogeneous Dirichlet boundary conditions.

Theorem 2.1. *The aforementioned assumptions* (AA)*&*(DP) *imply*

$$(1 + \delta_{hH})^{-1} \eta \leq \left\| e \right\| \leq \left(\eta + \min_{v_H \in u_{DH} + V_2} \left\| u - v_H \right\| \right) / \sqrt{1 - q^2}. \tag{2.5}$$

Proof. The efficiency of η (lower bound) follows with the definition in (AA) and the triangle inequality. Indeed,

$$\eta \leq \left\| e \right\| + \delta_{hH} \min_{v_h \in u_{\mathrm{Dh}} + V_1} \left\| u - v_h \right\| \leq (1 + \delta_{hH}) \left\| e \right\|.$$

To show the reliability of η (upper bound), define $e_H := G_2 e \in V_2$ as the Riesz representation of e in the sense that

$$a(e - e_H, v_H) = 0 \qquad \text{for all } v_H \in V_2.$$

The definition of q in (DP) implies

$$\left\| e_H \right\|^2 = a(e, e_H) = \min_{v_h \in V_1} a(e, e_H - v_h) \leq q \left\| e \right\| \left\| e_H \right\|.$$

That is,

$$\left\| e_H \right\| \leq q \left\| e \right\|. \tag{2.6}$$

The Pythagoras theorem yields

$$\left\| e \right\|^2 = \left\| e - e_H \right\|^2 + \left\| e_H \right\|^2 \leq \left\| e - e_H \right\|^2 + q^2 \left\| e \right\|^2.$$

The orthogonality implies for all $v_H \in V_2$ that

$$\left\| e - e_H \right\|^2 = a(e - e_H, e - v_H) \leq \left\| e - e_H \right\| \left\| e - v_H \right\|.$$

The combination of the previous estimates leads to

$$(1 - q^2)^{1/2} \left\| e \right\| \leq \left\| e - e_H \right\| \leq \min_{v_H \in V_2} \left\| e - v_H \right\|.$$

The split $e - v_H = u - v_H{}' - (u_h - v_H{}'')$ for $v_H{}', v_H{}'' \in u_{\mathrm{DH}} + V_2$, and a triangle inequality proves

$$\min_{v_H \in V_2} |||e - v_H||| \le |||u - v_H{}'||| + |||u_h - v_H{}''||| \quad \text{for all } v_H{}', v_H{}'' \in u_{\mathrm{DH}} + V_2.$$

Since the test functions $v_H{}'$ and $v_H{}''$ are arbitrary, this leads to

$$(1 - q^2)^{1/2} |||e||| \le \eta + \min_{v_H \in u_{\mathrm{DH}} + V_2} |||u - v_H||| \,.$$

This concludes the proof. □

Remark 2.1. The discrete property (DP) was verified in [CP07] for a sufficiently large (but unknown) number of uniform red-refinements k. In fact, for $h/H = 2^k$, the local inverse inequality

$$\|H \nabla_H v\|_{L^2(\Omega)} \le c_{\mathrm{inv}} \|v\|_{L^2(\Omega)} \qquad \text{for all } v \in P_1(\mathcal{T}_H)$$

holds with some constant c_{inv} which only depends on the angles in the triangulation $\mathcal{T}_H$ where ∇_H denotes the piecewise gradient operator. Together with a standard interpolation error estimate [Bra07, BS08, CGR12]

$$\|\nabla(v - I_1 v)\|_{L^2(\Omega)} \le C(\mathcal{T}) \left\|h D^2 v\right\|_{L^2(\Omega)} \quad \text{for } v \in C(\overline{\Omega}) \cap H^2(\mathcal{T}_h),$$

this proves

$$q := \max_{v_H \in (u_{\mathrm{DH}} + V_2)\setminus\{0\}} \min_{v_h \in u_{\mathrm{Dh}} + V_1} \frac{|||v_H - v_h|||}{|||v_H|||} \le c_{\mathrm{inv}} C(\mathcal{T}) 2^{-k}.$$

Hence, the upper bound is strictly smaller than 1 for k sufficiently large. However, the appropriate values for k are unclear. Numerical evidence in [CP07] supports that even $k = 1$ might be sufficient. Some computer-supported argument shows that this is in fact true for a large class of meshes.

Theorem 2.2. *Assume a regular triangulation $\mathcal{T}_H$ of the domain $\overline{\Omega} \subset \mathbb{R}^2$ into triangles for which all inner angles are smaller than or equal to $\pi/2$. Then $q \le 3/4$ in* (DP) *and $\eta_h := |||(1 - I_2)u_h|||$ satisfies*

$$|||u - u_h||| \le \frac{4}{\sqrt{7}} \left(\eta_h + \min_{v_H \in u_{DH} + V_2} |||u - v_H||| \right).$$

An immediate consequence is the following error reduction for the Galerkin projection G_2 with respect to $u_{\mathrm{DH}} + V_2$.

Corollary 2.3 (Saturation of postprocessing)**.** *The postprocessing $G_2 u_h$ satisfies*

$$|||u - G_2 u_h|||^2 \le \frac{9}{16} |||u - u_h|||^2 + \min_{v_H \in u_{DH} + V_2} |||u - v_H|||^2 .$$

Proof. By orthogonality, for $e_H \equiv G_2(u - u_h)$ it holds

$$|||u - G_2 u_h|||^2 = |||u - G_2 u + e_H|||^2 = |||e_H|||^2 + \min_{v_H \in u_{\mathrm{DH}} + V_2} |||u - v_H|||^2 .$$

This and (2.6) with $q \le 3/4$ conclude the proof. □

Reliability of η is proved if $q < 1$ holds in (DP). For the nodal interpolation operator I_1, define

$$\varkappa := \max_{v \in P_2(T)} \frac{\|\!|v - I_1 v|\!\|_T}{\|\!|v|\!\|_T} < 1 \quad \text{for all } T \in \mathcal{T}_H. \tag{2.7}$$

In fact, the following proof shows that $\varkappa \leq 3/4$ for $\max \sphericalangle(\mathcal{T}_\ell) \leq \pi/2$.

Proof of Theorem 2.2. The computer-supported proof follows in six steps, where T denotes some triangle and $\|\!|\cdot|\!\|_T := \|\nabla \cdot\|_{L^2(T)}$.

Step 1: Reduction to finite-dimensional eigenvalue problem

Let $\varphi_1, \varphi_2, \varphi_3$ denote the first-order nodal basis functions of the three vertices of the triangle T and define the edge-bubble functions

$$b_j := \varphi_{j+1}\varphi_{j-1} - \frac{1}{3}(\varphi_{j+1} + \varphi_{j-1}) + \frac{5}{36} \qquad \text{for } j = 1, 2, 3. \tag{2.8}$$

Here, the subindex $j \pm 1$ is to be understood in the sense $(j \pm 1 \mod 3) + 1$.

Lemma 2.4. *On any triangle $T \in \mathcal{T}_H$ it holds*

$$\max_{v \in P_2(T)/\mathbb{R}} \frac{\|\!|v - I_1 v|\!\|_T}{\|\!|v|\!\|_T} = \max_{v \in \operatorname{span}\{b_1, b_2, b_3\} \setminus \{0\}} \frac{\|\!|v - I_1 v|\!\|_T}{\|\!|v|\!\|_T}.$$

Proof. Given any $v \in P_2(T)/\mathbb{R}$ with $\|\!|v - I_1 v|\!\|_T > 0$ and $\|\!|v|\!\|_T > 0$, suppose $\int_T v \, dx = 0$ and set $M := |T|^{-1} \int_T \nabla v \, dx \in \mathbb{R}^2$. Then $w(x) := v(x) - M \cdot (x - \operatorname{mid}(T))$ for $x \in T$ satisfies $v - I_1 v = w - I_1 w$ and (by orthogonality $\nabla v - M \perp \mathbb{R}^2$)

$$\|\!|v|\!\|_T^2 = \|\!|w|\!\|_T^2 + |M|^2 \, |T| \geq \|\!|w|\!\|_T^2 .$$

Consequently,

$$\frac{\|\!|v - I_1 v|\!\|_T}{\|\!|v|\!\|_T} \leq \frac{\|\!|w - I_1 w|\!\|_T}{\|\!|w|\!\|_T} \leq \max_{u \in U \setminus \{0\}} \frac{\|\!|u - I_1 u|\!\|_T}{\|\!|u|\!\|_T}$$

for $U := \{u \in P_2(T) \mid \int_T u \; dx = 0, \; \int_T \nabla u \; dx = 0\}$. A direct calculation with (2.8) proves that b_1, b_2, b_3 belong to U and form a basis of U. Since $v \in P_2(T)/\mathbb{R}$ is arbitrary, this proves the asserted inequality "$\leq$" of the lemma. The inequality "$\geq$" is obvious from $U \subseteq P_2(T)/\mathbb{R}$. $\square$

Step 2: An eigenvalue problem on the reference triangle

It is instructive to first examine the eigenvalue problem on the reference triangle $T_{\text{ref}} := \operatorname{conv}\{(0,0), (1,0), (0,1)\}$. Lemma 2.4 leads to the maximisation of

$$\frac{\|\!|x_1(b_1 - I_1 b_1) + x_2(b_2 - I_1 b_2) + x_3(b_3 - I_1 b_3)|\!\|_T^2}{\|\!|x_1 b_1 + x_2 b_2 + x_3 b_3|\!\|_T^2} = \frac{x \cdot Ax}{x \cdot Bx} \tag{2.9}$$

for $x \in \mathbb{R}^3$ while the 3×3 symmetric positive definite matrices A and B read

$$A_{jk} := \int_T \nabla(b_j - I_1 b_j) \cdot \nabla(b_k - I_1 b_k)\, dx \qquad \text{for } j,k = 1,2,3,$$
$$B_{jk} := \int_T \nabla b_j \cdot \nabla b_k \, dx \qquad \text{for } j,k = 1,2,3.$$

The computation of the matrices yields

$$A_{\text{ref}} := \frac{1}{48}\begin{pmatrix} 2 & -1 & -1 \\ -1 & 2 & 0 \\ -1 & 0 & 2 \end{pmatrix} \quad \text{and} \quad B_{\text{ref}} := \frac{1}{36}\begin{pmatrix} 2 & -1 & -1 \\ -1 & 4 & 0 \\ -1 & 0 & 4 \end{pmatrix}.$$

The evaluation of (2.9) amounts to solving the generalised eigenvalue problem $A_{\text{ref}}x = \lambda B_{\text{ref}}x$ the largest eigenvalue of which represents the upper bound q. This leads to the eigenvalues $3/4,\ 3/8,\ 1/4$, which proves (2.7) with $\varkappa = 3/4$ on the reference triangle.

Step 3: Eigenvalue problem on arbitrary triangle

Without loss of generality, suppose $T = \operatorname{conv}\{(0,0),(1,0),(a,b)\}$ for $0 < a, b \leq 1$. With $\alpha := a - a^2 - b^2$ and $\beta := a^2 + b^2$. The matrices A and B read

$$\begin{aligned} A &= \frac{1}{48}\begin{pmatrix} 1-\alpha & \alpha & a-1 \\ \alpha & 1-\alpha & -a \\ a-1 & -a & 1-\alpha \end{pmatrix}, \\ B &= \frac{1}{36}\begin{pmatrix} \beta + a + 1 & a - \beta & a-1 \\ a-\beta & \beta - 3a + 3 & -a \\ a-1 & -a & 3\beta - 3a + 1 \end{pmatrix}. \end{aligned} \tag{2.10}$$

Some direct calculations prove that

$$A\begin{pmatrix}1 & 1 & 1\end{pmatrix}^T = 1/4\, B\begin{pmatrix}1 & 1 & 1\end{pmatrix}^T$$

independent of the parameters α and β.

Step 4: Evaluation of the eigenvalues

The eigenvalue problem of step 3 allows a closed form solution of the three eigenvalues. As seen from above numerically, the smallest of those is $\lambda_1 = 1/4$. The other two eigenvalues λ_2, λ_3 are complicated polynomial functions of the parameters a and b. We provide the symbolical calculations in the form of a MuPAD session (the symbolical toolbox of Matlab) as supplementary material on request.

Figure 2 shows the graph of the largest eigenvalue $\lambda_3(a,b)$ for $0 \leq a, b \leq 1$ which corresponds to the triangles $T = \operatorname{span}\{(0,0),(1,0),(a,b)\}$. The plot on the right-hand side depicts the clipped eigenvalue $\hat{\lambda}_3(a,b) := \min\{\lambda_3(a,b), 1\}$ for better visualisation of the crucial area

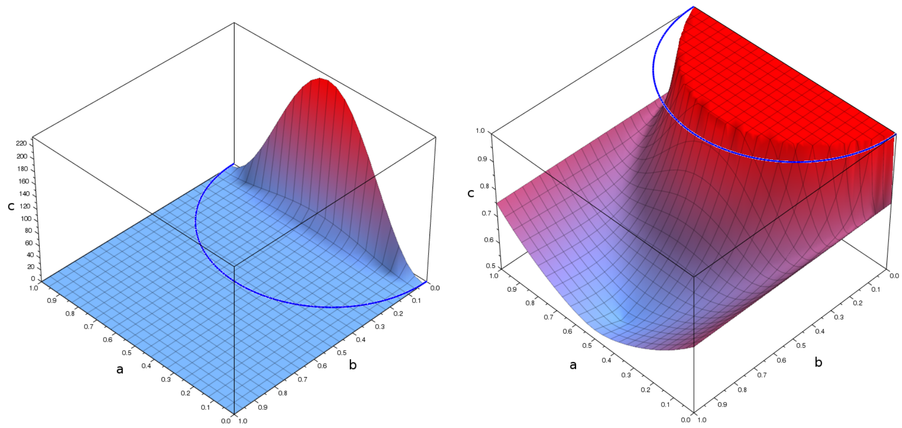

Figure 2: Largest eigenvalue $\lambda_{\max}$ for generalised eigenvalue problem (2.9) with matrices (2.10) on arbitrary triangles $\operatorname{conv}\{(0,0),(1,0),(a,b)\}$, $0 < a,b \leq 1$ [left] and clipped graph $(a,b) \mapsto \min\{\lambda_{\max}(a,b),1\}$ [right].

along the half circle around $(1/2,0)$ which is indicated with a function value of 1. It is apparent that for all coordinates outside of the half circle, function values smaller than 1 are assumed. In fact, since λ_3 is $3/4$ along the half circle (see Step 5) and the numerical experiments suggest that the largest eigenvalue is strictly smaller than $3/4$ with triangles for which all inner angles are smaller than or equal to $\pi/2$.

Step 5: Discussion of special cases

The initial examination of the reference triangle also has a practical relevance since the result applies to meshes consisting of squares which are halved diagonally.

For the curve defined by $(a-1/2)^2+b^2=1/4$, i.e. the circle with center $(0,1/2)$ in the upper half plane, the solution of the eigenvalue problem greatly simplifies. Note that by this we define the triangles which are right-angled at (a,b). The substitution of b leads to the same eigenvalues as on the reference triangle, independent of a.

Step 6: Finish of the proof

The result of step 4 carries over to arbitrary triangles since rotation, scaling, and translation do not change the eigenvalues. Thus, for appropriate triangulations, $q=3/4$ in (DP). The stated result immediately follows from Theorem 2.1. $\square$

3 Equivalence of Norms

This section establishes the equivalence of the error estimator η_h of the preceding section and some norms defined by edge jumps.

3.1 Equivalence of η_h with edge-jumps

We first show the equivalence of the error estimator η_h with the norm of the jumps on some but not all interior edges. Consider a triangle $T \in \mathcal{T}_H$ and its red-refinement $\mathrm{red}(T) \subseteq \mathcal{T}_h$ with interior edges $\{F_1, F_2, F_3\} =: \mathcal{F}(T)$ and degrees of freedom $\alpha_T := (\alpha_1, \dots, \alpha_6)$ depicted in Figure 3. Let $\varphi_T := (\varphi_1, \dots, \varphi_6)$ denote the nodal quadratic basis functions with respect to the nodes $x_1, \dots, x_6 \in \mathcal{N}_h$. Recall V_1 and V_2 from (2.2) and the associated interpolation operators I_1 and I_2.

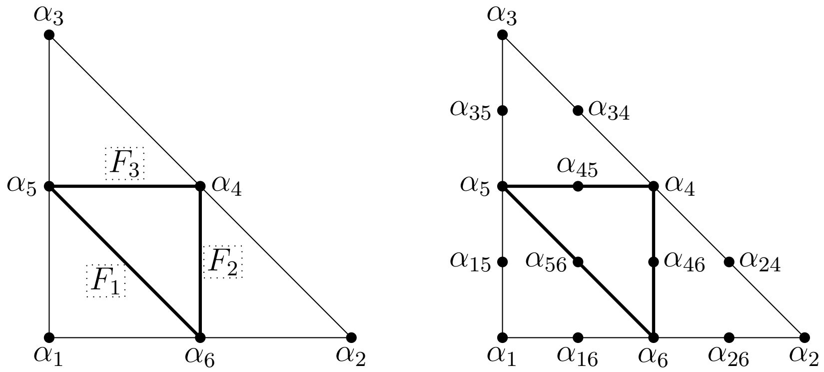

Figure 3: Degrees of freedom $\alpha_1, \dots, \alpha_6$ of a P_2 triangular element $T \in \mathcal{T}_H$ with indicated interior edges $\mathcal{F}(T) = \{F_1, F_2, F_3\}$ after red-refinement of T [left] and degrees of freedom for $P_2(\mathrm{red}(T))$ [right].

Proposition 3.1. *On any triangle $T \in \mathcal{T}_H$,*

$$\|v_h\|_{\mathcal{F}(T)} := \left(\sum_{j=1}^{3} |F_j| \left\| \left[\partial v_h / \partial \nu_{F_j} \right]_{F_j} \right\|^2_{L^2(F_j)} \right)^{1/2}$$

defines a semi-norm for $v_h \in V_1 + V_2$ and satisfies the equivalence

$$\eta_T(v_h) := \|\!|(1 - I_2)v_h|\!\|_T \approx \|(1 - I_2)v_h\|_{\mathcal{F}(T)}.$$

Proof. The assertion is an equivalence of the semi-norms $\|\!|\bullet|\!\|_T$ and $\|\bullet\|_{\mathcal{F}(T)}$ in the three-dimensional vector space

$$V_3 := (1 - I_2)(V_1 + V_2)|_T = (1 - I_2)V_1|_T.$$

Given any $v_3 \in V_3$, there exists $v_1 \in V_1|_T$ with $v_3 = (1 - I_2)v_1|_T$. In case $\|\!|v_3|\!\|_T = 0$, $v_3 \in P_1(T)$ with $v_3(x_j) = 0$ for all $j = 1, \dots, 6$. Therefore, $v_3 \equiv 0$.
In case $\|v_3\|_{\mathcal{F}(T)} = 0$, ∇v_3 has no jumps in normal direction along F_j for $j = 1, 2, 3$. Since there are no jumps in tangential direction on all F_j, ∇v_3 is continuous on T. Hence, ∇v_1 is constant on T which implies that $v_1 \in P_1(T)$. From $I_2 v_1 = v_1$ it follows that $v_3 = (1 - I_2)v_1 \equiv 0$.
Since $\|\!|\bullet|\!\|_T$ and $\|\bullet\|_{\mathcal{F}(T)}$ are equivalent norms in the finite-dimensional space V_3, the assertion $c_1 \|\!|\bullet|\!\|_T \le \|\bullet\|_{\mathcal{F}(T)} \le C_2 \|\!|\bullet|\!\|_T$ follows with equivalence constants c_1 and C_2 which may depend on T. A scaling argument reveals that these constants may in fact depend of the shape of the triangle but not on the size $h_T := \mathrm{diam}(T)$. $\square$

Corollary 3.2. *For $\mathcal{F}_{\text{int}} := \{F_j : F_j \in \mathcal{F}(T) \mid T \in \mathcal{T}\}$, it holds*

$$\eta_h^2 \equiv |||(1-I_2)u_h|||^2 \approx \sum_{F\in\mathcal{F}_{\text{int}}} |F|\, \|[\partial u_h/\partial\nu_F]_F\|^2_{L^2(F)}\,.$$

Proof. This follows from the observation that $\nabla I_2 u_h$ is continuous along any interior edge $F_j \in \mathcal{F}_{\text{int}}$. Hence,

$$\|(1-I_2)u_h\|_{\mathcal{F}(T)} = \|u_h\|_{\mathcal{F}(T)} \quad \text{for } T\in\mathcal{T}.$$

This and Proposition 3.1 lead to

$$\eta_h^2 = \sum_{T\in\mathcal{T}} \eta_T^2(u_h) \approx \sum_{T\in\mathcal{T}} \|u_h\|^2_{\mathcal{F}(T)}\,. \qquad \square$$

Corollary 3.3. *It holds*

$$\eta_h \lesssim |||u-u_h||| + \operatorname{osc}(f,\mathcal{T}_h).$$

Proof. This follows from Corollary 3.2 and the well-established efficiency of the jump residuals, e.g., see [Ver96]. $\square$

3.2 Refined explicit residual-based a posteriori error control

It was shown in [CV99] that the error $u-u_h$ is bounded by the edge jumps of $u_h \in u_{\text{Dh}} + V_1$ plus nodal-patch data oscillations. The key theorem of this section extends this result by a restriction to the interior edges $\mathcal{F}_{\text{int}}$. Moreover, it enables the control of the higher-order term in Theorem 2.2 by η_h and data oscillations.

Throughout this section we assume that each triangle in $\mathcal{T}_H$ has at least one vertex in Ω. We recall the main result of [CV99] (also see [Car99, Car04]) which is generalised by Corollary 3.6 and used in the proof of Theorem 3.5.

Theorem 3.4 ([CV99]). *For the exact solution u and the discrete solution $u_h \in u_{Dh}+V_1$ to* (2.3) *it holds*

$$|||u-u_h|||^2 \lesssim \sum_{F\in\mathcal{E}_h(\Omega)} |F|\, \|[\partial u_h/\partial\nu_F]_F\|^2_{L^2(F)} + \operatorname{osc}^2(f,\mathcal{N}_h).$$

Theorem 3.5. *The exact solution u, the discrete solution $u_h \in u_{Dh}+V_1$ and η_h from Theorem 2.2 satisfy*

$$|||u-u_h||| \lesssim \left(\sum_{F\in\mathcal{F}_{int}} |F|\, \|[\partial u_h/\partial\nu_F]_F\|^2_{L^2(F)}\right)^{1/2} + \operatorname{osc}(f,\mathcal{N}_h).$$

Remark 3.1. The oscillations are based on the coarse patches ω_z for $z\in\mathcal{N}_H$. The assertion remains valid if $\operatorname{osc}(f,\{\omega_z \mid z\in\mathcal{N}_H\})$ is replaced by the oscillations $\operatorname{osc}(f,\{\omega_z^h \mid z\in\mathcal{N}_h\})$ with respect to the fine triangulation. This is seen from an equivalence of norms argument that leads to

$$\operatorname{osc}(f,\omega_z) \lesssim \operatorname{osc}(f,\{\omega_y^h \mid y\in\mathcal{N}_H(\omega_z)\})$$

for any $z\in\mathcal{N}_H$ and interior nodes $\mathcal{N}_h(\omega_z)$ of ω_z in the fine triangulation. (For a proof, consider f piecewise constant first.)

Before the proof of Theorem 3.5 concludes this subsection, some corollaries are in order for which we define the skeleton of $\mathcal{T}_h$ by $\mathcal{F} := \{F \in \mathcal{E}_h(\Omega) \mid \forall E \in \mathcal{E}_H, F \not\subseteq E\}$.

Corollary 3.6. *The exact solution u and the discrete solution $u_h \in u_{Dh} + V_1$ satisfy*

$$\|u - u_h\| \lesssim \eta_h + \operatorname{osc}(f, \mathcal{N}_h).$$

Proof. This follows from Theorem 3.5 and Corollary 3.2. □

The following corollary justifies to neglect the higher-order term in Theorem 2.2 even pre-asymptotically at the expense of patch-oscillations and another constant.

Corollary 3.7. *The discrete solution $u_h \in u_{Dh}+V_1$ and the error estimator η_h from Theorem 2.2 satisfy*

$$\min_{v_H \in u_{DH}+V_2} \|u - v_H\| \lesssim \eta_h + \operatorname{osc}(f, \mathcal{N}_h).$$

Proof. Since $I_2 u_h \in u_{\mathrm{DH}} + V_2$, a triangle inequality and Theorem 3.5 imply

$$\begin{aligned}\min_{v_H \in u_{\mathrm{DH}}+V_2} \|u - v_H\| \leq \|u - I_2 u_h\| &\leq \|u - u_h\| + \eta_h \\ &\lesssim \eta_h + \operatorname{osc}(f, \mathcal{N}_h).\square\end{aligned}$$

The reliability constant is hidden in the notation "$\lesssim$".

Small data oscillations bound δ_{hH}.

Corollary 3.8. *The exact solution u and the discrete solution $u_h \in u_{Dh} + V_1$ satisfy*

$$\delta_{hH} \lesssim 1 + \operatorname{osc}(f, \mathcal{N}_h) / \|u - u_h\|.$$

Proof. Corollary 3.7 yields

$$\delta_{hH} = \frac{\min_{v_H \in u_{\mathrm{DH}}+V_2} \|u - v_H\|}{\min_{v_h \in u_{\mathrm{Dh}}+V_1} \|u - v_h\|} \lesssim \frac{\eta_h + \operatorname{osc}(f, \mathcal{N}_h)}{\|u - u_h\|}.$$

This and Corollary 3.3 conclude the proof. □

Proof of Theorem 3.5. The proof follows in three steps.

Step 1: Design of $\phi_1, \ldots, \phi_J$. Consider the patch ω_z of the interior node $z \in \mathcal{N}_H$ in Figure 4, which is the union of J triangles $\omega_z = \operatorname{int}(\bigcup_{j=1}^J T_j)$ with $T_j \in \mathcal{T}_H$ and $E_j := \operatorname{conv}\{z, P_j\}$ for $j = 1, \ldots, J$. We design functions $\phi_j \in V_1 \cap C_0(\omega_z)$ such that

$$\int_{\omega_z} \phi_j \, dx = 0 \quad \text{and} \quad |E_j|^{-1} \int_{E_j} \phi_k \, ds = \delta_{jk} \quad \text{for} \quad j = 1 \ldots J. \tag{3.1}$$

Such functions can be constructed explicitly with the nodal basis functions $\psi_j \in V_1$ in the fine triangulation $\mathcal{T}_h$ associated to $\operatorname{mid}(E_j)$ with $|E_k|^{-1} \int_{E_k} \psi_j \; ds = \delta_{jk}/2$ and $\psi_0 := \varphi_z -$

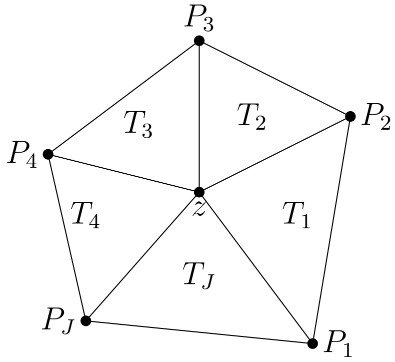

Figure 4: Patch ω_z in $\mathcal{T}_H$ for node $z \in \mathcal{N}_H$ with triangles $T_1, \ldots, T_J \in \mathcal{T}_H$ in the proof of Theorem 3.5.

$\sum_{j=1}^{J} \psi_j$. Here, $\varphi_z \in P_1(\mathcal{T}_H) \cap C(\omega_z)$ is the nodal basis function of the node $z \in \mathcal{N}_H$ with respect to the coarse triangulation $\mathcal{T}_H$. Then,

$$\int_{E_k} \psi_0 \, ds = 0 \qquad \text{and} \qquad |\omega_z|^{-1} \int_{\omega_z} \psi_0 \, dx = -1/6.$$

With $\alpha_j = 12\,|\omega_z|^{-1} \int_{\omega_z} \psi_j \, dx$, the function $\phi_j := 2\psi_j + \alpha_j \psi_0$ satisfies the first equation in (3.1). The second follows from the definition of ϕ_k along any edge E_j and $\int_{E_j} \phi_k \, ds = 2 \int_{E_j} \psi_k \, ds = \delta_{jk}\,|E_j|$.

Step 2: Two semi-norms. Let $\mathcal{E}_h(\omega_z)$ consist of all edges in the fine triangulation $\mathcal{T}_h$, which belong to $\overline{\omega_z}$ but do not lie on $\partial\omega_z$. Let $\mathcal{F}_{\text{int}}(\omega_z)$ be the set of all edges F in $\mathcal{E}_h(\omega_z)$ outside the skeleton $\bigcup \mathcal{E}_H$ of the coarse triangulation $\mathcal{T}_H$ in the sense that $F \not\subset E$ for any $E \in \mathcal{E}_H(\omega_z) := \bigcup\{E \in \mathcal{E}_H : z \in E\}$. In other words, the edges in $\mathcal{F}_{\text{int}}(\omega_z)$ are generated as interior new edges of triangles $K \in \mathcal{T}_H$ in the red-refinement of $\mathcal{T}_H$; cf. Figure 3 for an illustration on one triangle. For any $v_h \in V_1(\omega_z) := \{v_1|_{\omega_z} : v_1 \in V_1\}$, the expressions

$$\rho_1(v_h|_{\omega_z}) := \left(\sum_{F \in \mathcal{E}_h(\omega_z)} \| [\partial v_h / \partial \nu_F]_F \|_{L^1(F)}^2 \right)^{1/2} \quad \text{and} \tag{3.2}$$

$$\begin{aligned} \rho_2(v_h|_{\omega_z}) := &\left(\sum_{F \in \mathcal{F}_{\text{int}}(\omega_z)} \| [\partial v_h / \partial \nu_F]_F \|_{L^1(F)}^2 \right)^{1/2} \\ &+ \sum_{j=1}^{J} \left| \int_{\omega_z} \nabla \phi_j \cdot \nabla v_h \, dx \right| \end{aligned} \tag{3.3}$$

define two semi-norms on $V_1(\omega_z)$. The second semi-norm ρ_2 includes some (but not all) interior edges of the finer triangulation $\mathcal{T}_h$ and adds the functions $\phi_j \in P_1(\mathcal{T}_h) \cap C(\omega_z)$ associated with the edges of $\mathcal{E}_H(z)$ from (3.1). Proposition 3.1 asserts that the first term in the definition of $\rho_2(u_h|_{\omega_z})$ is equivalent to the error estimator $\eta_h(\omega_z) := \|\nabla(1 - I_2)u_h\|_{L^2(\omega_z)}$.

For the equivalence of ρ_1 and ρ_2, we first consider $u_h \in V_1$ with $\rho_1(v_h|_{\omega_z}) = 0$. It immediately follows that $v_h \in P_1(\omega_z)$ and the first term of $\rho_2(v_h|_{\omega_z})$ in (3.3) vanishes. An integration by parts and $[\nabla v_h]_{E_j} = 0$ lead to

$$\int_{\omega_z} \nabla\phi_j \cdot \nabla v_h \, dx = \int_{E_j} \left[\frac{\partial v_h}{\partial \nu_{E_j}}\right]_{E_j} \phi_j \, ds = 0. \tag{3.4}$$

Hence, the second term in (3.3) also vanishes and $\rho_2(v_h|_{\omega_z}) = 0$.
In case $u_h \in V_1$ satisfies $\rho_2(v_h|_{\omega_z}) = 0$, the vanishing first term in (3.3) implies that $v_h \in P_1(\mathcal{T}_H(z)) \cap C(\omega_z)$. The second term in (3.3) also vanishes and (with constant $[\nabla v_h]_{E_j} \in P_0(E_j;\mathbb{R}^2)$) (3.4) holds for $v_h \in P_1(\mathcal{T}_H(z))$. Hence, $[\nabla v_h]_{E_j} = 0$ on E_j for $j = 1,\dots,J$. This implies $v_h \in P_1(\omega_z)$ and so $\rho_1(v_h|_{\omega_z}) = 0$. A scaling argument reveals that the equivalence constants in $\rho_1 \approx \rho_2$ on $\{v_h|_{\omega_z} \mid v_h \in V_1\}$ factorised by $P_1(\omega_z) = \ker\rho_1 = \ker\rho_2$ do not depend on the patch sizes and solely depend on the shape of the triangles involved.

Step 3: Proof of Theorem 3.5. For $f_z := |\omega_z|^{-1}\int_{\omega_z} f \, dx$ and $\mathrm{osc}(f,\omega_z) := \mathrm{diam}(\omega_z)\,\|f - f_z\|_{L^2(\omega_z)}$, the discrete solution $u_h \in V_1$ to (2.3) and (3.1) followed by a Poincaré inequality lead to

$$\begin{aligned}\sum_{j=1}^{J}\left|\int_{\omega_z} \nabla u_h \cdot \nabla\phi_j \, dx\right| &= \sum_{j=1}^{J}\left|\int_{\omega_z} (f - f_z)\phi_j \, dx\right| \\ &\lesssim \mathrm{diam}(\omega_z)\,\|f - f_z\|_{L^2(\omega_z)} = \mathrm{osc}(f,\omega_z).\end{aligned}$$

Recall that $\mathcal{T}_H(z) := \{T \in \mathcal{T}_H \mid z \in \mathcal{N}(T)\}$. Step 2 leads to

$$\rho_1(u_h|_{\omega_z}) \approx \rho_2(u_h|_{\omega_z}) \lesssim \|u_h\|_{\mathcal{F}(\omega_z)} + \mathrm{osc}(f,\omega_z)$$

where $\|u_h\|_{\mathcal{F}(\omega_z)} := \left(\sum_{T\in\mathcal{T}_H(z)} \|u_h\|^2_{\mathcal{F}(T)}\right)^{1/2}$. The sum of all those interior patches with their finite overlap and the assumption that each triangle has at least one vertex in the interior of the domain results in

$$\begin{aligned}\mathrm{LHS} := \sum_{F\in\mathcal{E}_h(\Omega)} |F|\,\|[\partial u_h/\partial\nu_F]_F\|^2_{L^2(F)} &\lesssim \sum_{z\in\mathcal{N}_H(\Omega)} \rho_1^2(u_h|_{\omega_z}) \\ &\lesssim \|u_h\|^2_{\mathcal{F}_{\mathrm{int}}} + \sum_{z\in\mathcal{N}_H(\Omega)} \mathrm{osc}^2(f,\omega_z).\end{aligned}$$

Here and throughout,

$$\|u_h\|_{\mathcal{F}_{\mathrm{int}}} := \left(\sum_{T\in\mathcal{T}_H}\sum_{F\in\mathcal{F}(T)} |F|\,\|[\partial u_h/\partial\nu_F]_F\|^2_{L^2(F)}\right)^{1/2}.$$

Since Theorem 3.4 guarantees

$$|||u - u_h|||^2 \lesssim \mathrm{LHS} + \mathrm{osc}^2(f,\mathcal{N}_h),$$

the preceding estimate of LHS proves

$$|||u - u_h||| \lesssim \|u_h\|_{\mathcal{F}_{\mathrm{int}}} + \mathrm{osc}(f,\mathcal{N}_H).$$

Remark 3.1 shows $\mathrm{osc}(f,\mathcal{N}_H) \approx \mathrm{osc}(f,\mathcal{N}_h)$ and concludes the proof. $\square$

3.3 Piecewise averaging is reliable

This subsection is devoted to the proof that, surprisingly, *arbitrary local smoothing of the primal variable* $u_h \in u_{\mathrm{Dh}} + P_1(\mathrm{red}(T)) \cap C_D(\Omega)$ leads to a reliable error estimator. For this, we define the nonconforming distance on some triangulation $\mathcal{T}$ by

$$\mathrm{dist}_{\mathrm{NC}}(u_h, P_k(\mathcal{T})) := \left(\sum_{T\in\mathcal{T}} \mathrm{dist}^2_{|||\cdot|||_{\mathrm{T}}}(u_h, P_k(T))\right)^{1/2}$$

with the best-approximation error $\mathrm{dist}_{|||\cdot|||_{\mathrm{T}}}(u_h, P_k(T))$ of the orthogonal projection of u_h onto $P_k(T)$ with respect to the energy norm on $T \in \mathcal{T}$. The following main result holds for any polynomial degree k.

Theorem 3.9. *For any exact solution u and discrete solution $u_h \in u_{Dh} + P_1(\mathrm{red}(\mathcal{T})) \cap C_D(\Omega)$ and any $k \geq 0$, there exists some constant C_2 which depends on the inner angles in $\mathcal{T}$ and on k (but not on the mesh sizes or number of elements in $\mathcal{T}$) such that*

$$|||u - u_h||| \leq C_2 \left(\mathrm{dist}_{\mathrm{NC}}(u_h, P_k(\mathcal{T})) + \mathrm{osc}(f, \mathcal{N}_h)\right). \tag{3.5}$$

Proof. Define the seminorms ρ_3 and ρ_4 for each $T \in \mathcal{T}$ and $v_h \in C(T) \cap P_1(\mathrm{red}(T))$ by

$$\rho_3(v_h) := \sqrt{\sum_{F\in\mathcal{F}_{\mathrm{int(T)}}} |F| \, \|\partial v_h/\partial \nu_F\|^2_{L^2(F)}},$$
$$\rho_4(v_h) := \mathrm{dist}_{|||\cdot|||_{\mathrm{T}}}(v_h, P_k(T)).$$

Since $\rho_4(v_h) = 0$ implies $v_h \in P_k(T) \subseteq C^1(T)$, all the interior normal jumps disappear for v_h, i.e. $\rho_3(v_h) = 0$. This holds for $k = 0, 1, 2, \dots$ and allows an argument along an equivalence of norms to prove $\rho_3(v_h) \leq C(k)\rho_4(v_h)$ for all $v_h \in P_1(\mathrm{red}(T)) \cap C(T)$. A scaling argument shows that the constant $C(k)$ (possibly depending on the degree k) is independent of the size of the triangle T but may depend on a lower bound of the interior angles in T. Hence, the inequality $\rho_3^2(u_h|_T) \lesssim \rho_4^2(u_h|_T)$ holds for each $T \in \mathcal{T}$. The sum over all $T \in \mathcal{T}$ yields

$$\sum_{F\in\mathcal{F}_{\mathrm{int}}} |F| \, \|\partial u_h/\partial \nu_F\|^2_{L^2(F)} \lesssim \sum_{T\in\mathcal{T}} \mathrm{dist}^2_{|||\cdot|||_T}(u_h, P_k(T)).$$

This and Theorem 3.4 conclude the proof. □

Remark 3.2. Several remarks are in order to elucidate the key point of the theorem and put it into perspective with previous results.

(1) Theorem 3.5 is a refinement and generalisation of the main result in [CV99] given by Theorem 3.4. The new result states for $\mathcal{T} = \mathrm{red}(\mathcal{T}_H)$ that only a subset of edges (i.e. the interior edges for any coarse triangle $K \in \mathcal{T}_H$) are required in the error estimator.

(2) An elementwise inverse estimate allows the control of

$$\mathrm{dist}_{\mathrm{NC}}(u_h, P_k(\mathcal{T})) \approx \min_{v_h\in P_k(\mathcal{T})} \left\|h_{\mathcal{T}}^{-1}(u_h - v_h)\right\|.$$

The proof considers any $K \in \mathcal{T}$ with $u_h|_K \in P_1(\mathrm{red}(\mathcal{T})) \cap C(\mathcal{T})$ and two seminorms ρ_4 and $\rho_5(u_h|_K) := h_k^{-1} \min_{v_k\in P_k(K)} \|u_h - v_k\|_{L^2(K)}$.

(3) Opposite to other hierarchical error estimators, no saturation assumption is required throughout this paper.

(4) The efficiency of the error estimator can be derived easily in two different ways. First, the error estimator η_h was shown to be efficient. Since the norm subject to the inner edges is equivalent to η_h (see Subsection 3.1) and thus is also equivalent to the error estimator in Theorem 3.9. Then, efficiency is immediate.

 Second, efficiency can be shown by projection of the locally smoothed functions onto the conforming space $P_k(\mathcal{T}_H)$. Since the conforming error estimator is known to be efficient and since it results in larger values than the nonconforming error estimator, efficiency of (3.5) is proved.

(5) The work [FLOP10] considers mesh-refinement on the level ℓ with respect to some related quantities μ_ℓ and $\tilde{\mu}_\ell$ with

$$\mathrm{dist}_{\mathrm{NC}}(u_\ell, P_1(\mathcal{T})) \leq \|\nabla u_\ell - \Pi_\ell \nabla u_\ell\| =: \tilde{\mu}_\ell \leq \mu_\ell.$$

 Therefore, this work provides reliability of the error estimators in [FLOP10] even for pure red-refinements.

4 Numerical Experiments

This section is devoted to the practical performance of the presented a posteriori error estimators and the higher-order properties as well as the observed efficiency indices. In each iteration step, the adaptive algorithm evaluates the local error contributions of η_h subject to the numerical solution u_h of (2.1) and selects a minimal set $\mathcal{M} \subset \mathcal{T}$ such that $\Theta {\eta_h}^2 \leq {\eta_h}^2(\mathcal{M})$ (Dörfler or bulk marking) with $\Theta = 0.3$. The efficiency is measured by the efficiency index

$$\mathrm{eff}_{\eta_h} := 4\eta_h/(\sqrt{7}\,|\!|\!|e|\!|\!|). \tag{4.1}$$

We neglect the higher-order term of Theorem 2.2 since it is controlled by η_h and oscillations as shown in Corollary 3.7. Consequently, the estimates are no longer guaranteed error bounds.

4.1 Minimal cross grid of square domain

The introductory example of Subsection 1.4 states the very good performance of the hierarchical error estimator even in the pre-asymptotic case on the coarsest possible mesh of the square domain. Figure 1 depicts the coarse mesh $\mathcal{T}_H$ (left) and the red-refinement $\mathcal{T}_h = \mathrm{red}(\mathcal{T}_H)$ (right). The respective spaces V_2 and V_1 have only the center degree of freedom α_5. To evaluate the error estimator $\eta_h(u_h) = |\!|\!|(1 - I_2)u_h|\!|\!|$, only the triangles T_3 and T_4 have to be considered due to symmetry. The shape function $\psi_5 \in V_2$ associated with α_5 is given by $\psi_5(x, y) := 4xy$, the P_1 shape functions $\varphi_3, \varphi_4 \in V_1$ are defined by $\varphi_3(x, y) := 2y$ and $\varphi_4(x, y) := 2x +$

$2y-1$. An integration of the difference of the respective P_1 and P_2 shape functions on the two triangles yields

$$
\begin{aligned}
E_3 &:= \int_{T_3} |\nabla(\psi_5 - \varphi_3)|^2 dx \\
&= 4 \int_{1/2}^{1} \int_{0}^{1-x} \left(4x^2 - 4x + 4y^2 + 1\right)\, dy\, dx = 1/6
\end{aligned}
$$

and similarly for triangle T_4

$$
\begin{aligned}
E_4 &:= \int_{T_4} |\nabla(\psi_5 - \varphi_4)|^2 dx \\
&= 8 \int_{0}^{1/2} \int_{1/2-x}^{1/2} \left(2x^2 - 2x + 2y^2 - 2y + 1\right)\, dy\, dx = 1/6.
\end{aligned}
$$

The solution $u_h \in P_1(\mathrm{red}(\mathcal{T}_H))$ for the model problem with homogeneous Dirichlet boundary conditions is given by $\alpha_5 = 1/16$. We sum up the integrals to obtain the error bound

$$
\begin{aligned}
\|u - u_h\| &\leq C_{\mathrm{rel}} \eta_h + \text{h.o.t.} = C_{\mathrm{rel}} \alpha_5 \sqrt{4E_3 + 2E_4} + \text{h.o.t.} \\
&= 4/\sqrt{7}\alpha_5 + \text{h.o.t.} = 0.0945 + \text{h.o.t.}
\end{aligned}
$$

4.2 Waterfall example

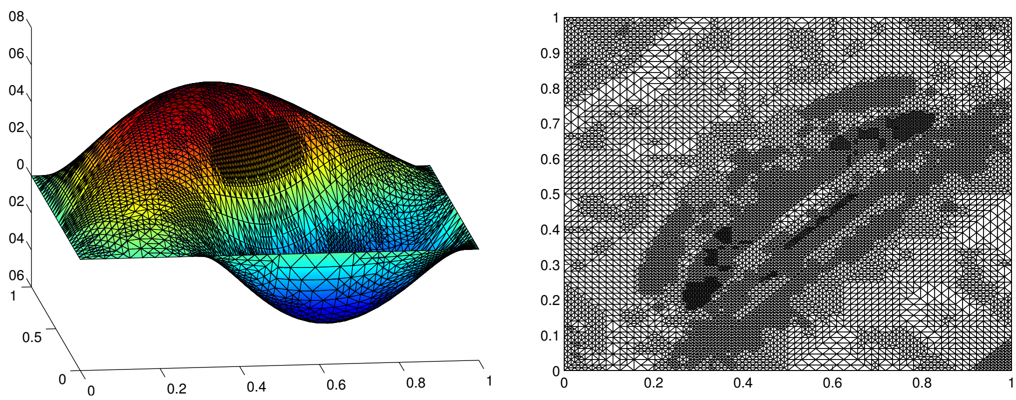

Figure 5: P_1 solution of the waterfall problem of Section 4.2 (left) and adaptively refined grid (right).

We choose f in (2.1) according to the exact solution of the *waterfall problem*

$$
u(x, y) = xy(1-x)(1-y)\,\mathrm{atan}\left(10\sqrt{(x-5/4)^2 + (y+1/4)^2} - 1\right)
$$

on the square domain $\Omega := (0,1)^2$ with zero boundary condition on $\partial\Omega$. The solution exhibits a steep gradient inside the domain in diagonal direction shown in Figure 5. The adaptive algorithm produces a refined grid along the edge of the “waterfall” and the energy norm of the error is $O(h)$ for uniform and adaptive refinement as can be seen in Figure 6.

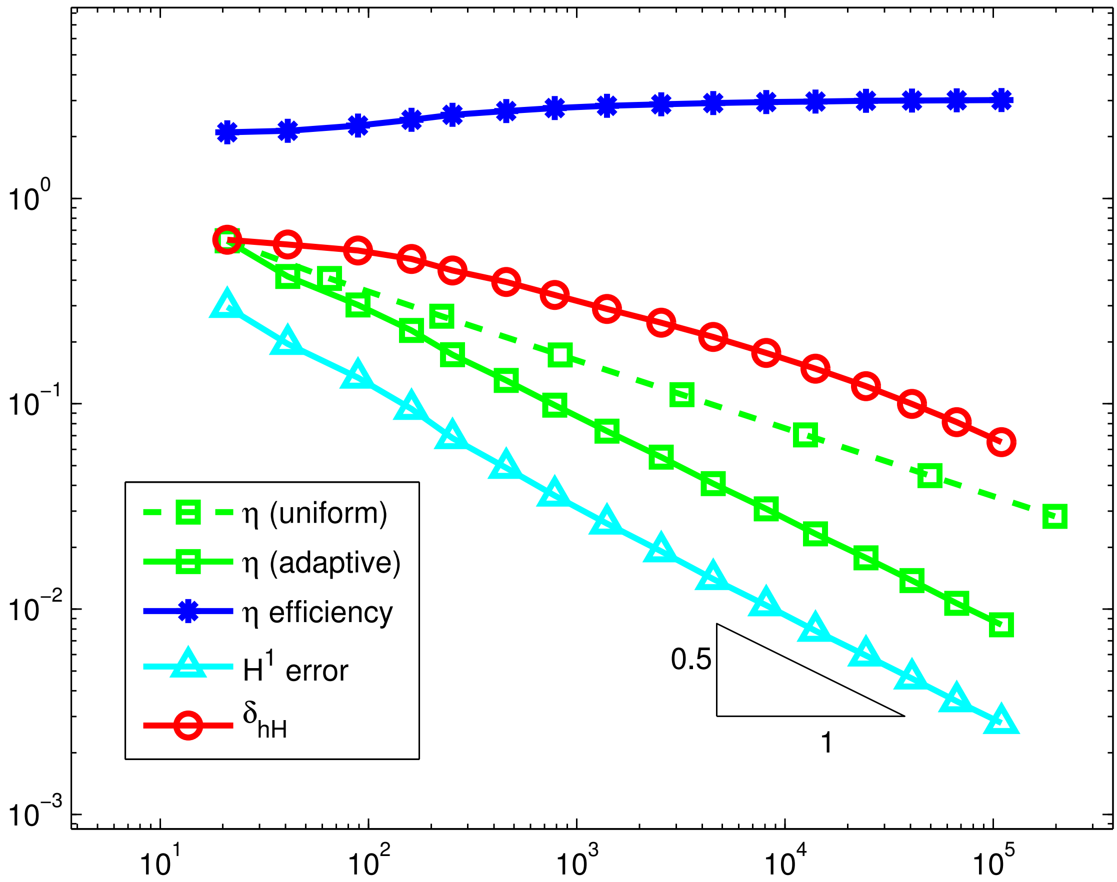

Figure 6: Estimator η_h of Theorem 2.2, δ_{hH} (AA), energy error and efficiency index (4.1) for waterfall problem on square for adaptive and uniform refinements.

4.3 L-shaped domain

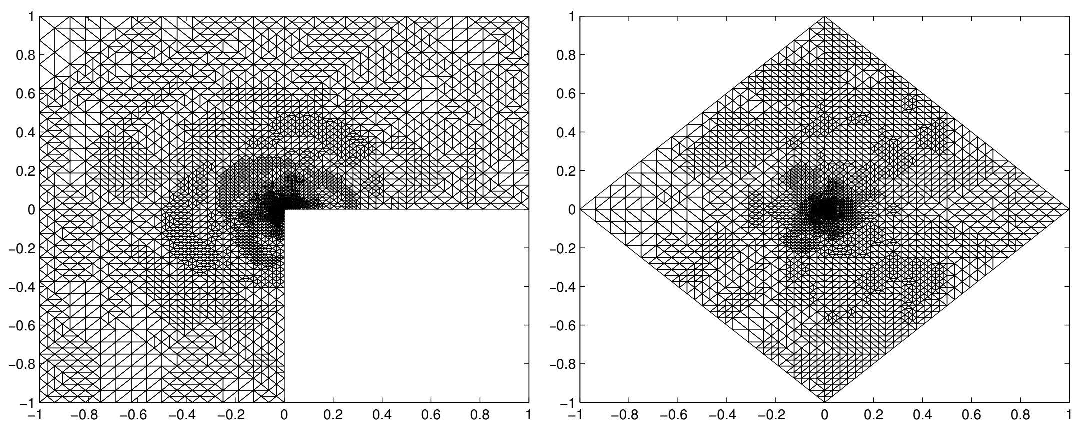

Figure 7: Adaptively refined L-shaped domain of Section 4.3 (left) and slit domain of Section 4.4 (right) which show strong refinement at the singularities of the solutions.

On the L-shaped domain $\Omega := (-1,1)^2 \setminus [-1,0]^2$ the model problem(2.1) is evaluated with f according to the exact solution

$$u = r^{2/3}\sin(2\varphi/3).$$

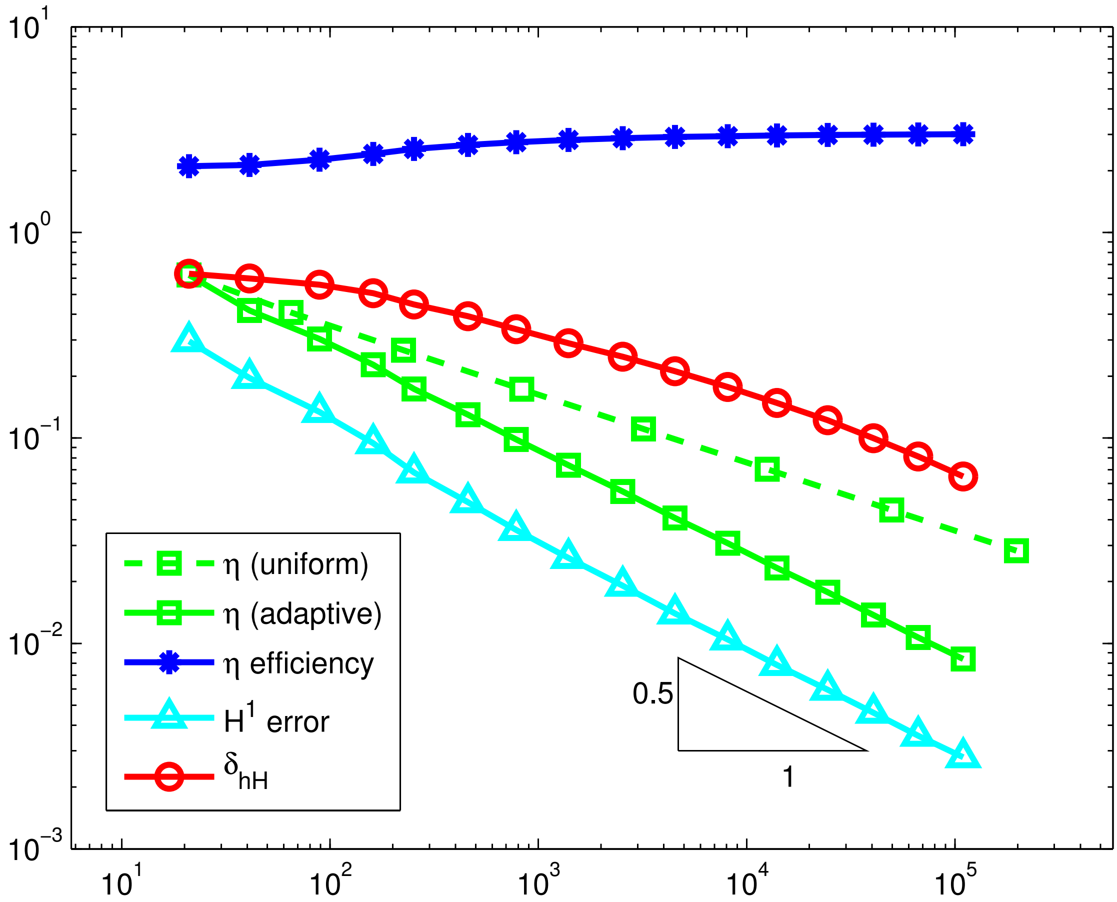

Figure 8: Estimator η_h, δ_{hH}, energy error and efficiency index for solution with singularity at re-entrant corner of L-shaped domain of Section 4.3 for adaptive and uniform refinements.

Since the solution exhibits a singularity at the origin, the energy norm of the error is of reduced order $O(h^{2/3})$ when uniform refinement is used. The full convergence rate can be regained when applying an adaptive refinement procedure based on the presented a posteriori error estimator. An indication for the inefficiency of the uniform refinement also can be seen when examining the plots of δ_{hH} in Figure 8. Clearly, the term is not of higher-order and the refinement process thus is not capable to adequately improve the approximation.

An adaptively refined mesh based on the hierarchical error estimator is shown in Figure 7 (left). Clearly, the refinement is concentrated around the singularity of the solution at the re-entrant corner at the origin.

4.4 Slit domain

On the domain $\Omega := (-1,1)^2 \setminus ([0,1] \times \{0\})$ the model problem (2.1) is evaluated with f according to the exact solution

$$u = r^{1/2} \sin\left(\frac{1}{2}\varphi\right) - \frac{1}{2}\left(r\sin(\varphi)\right)^2$$

with zero boundary condition on $\partial\Omega$.

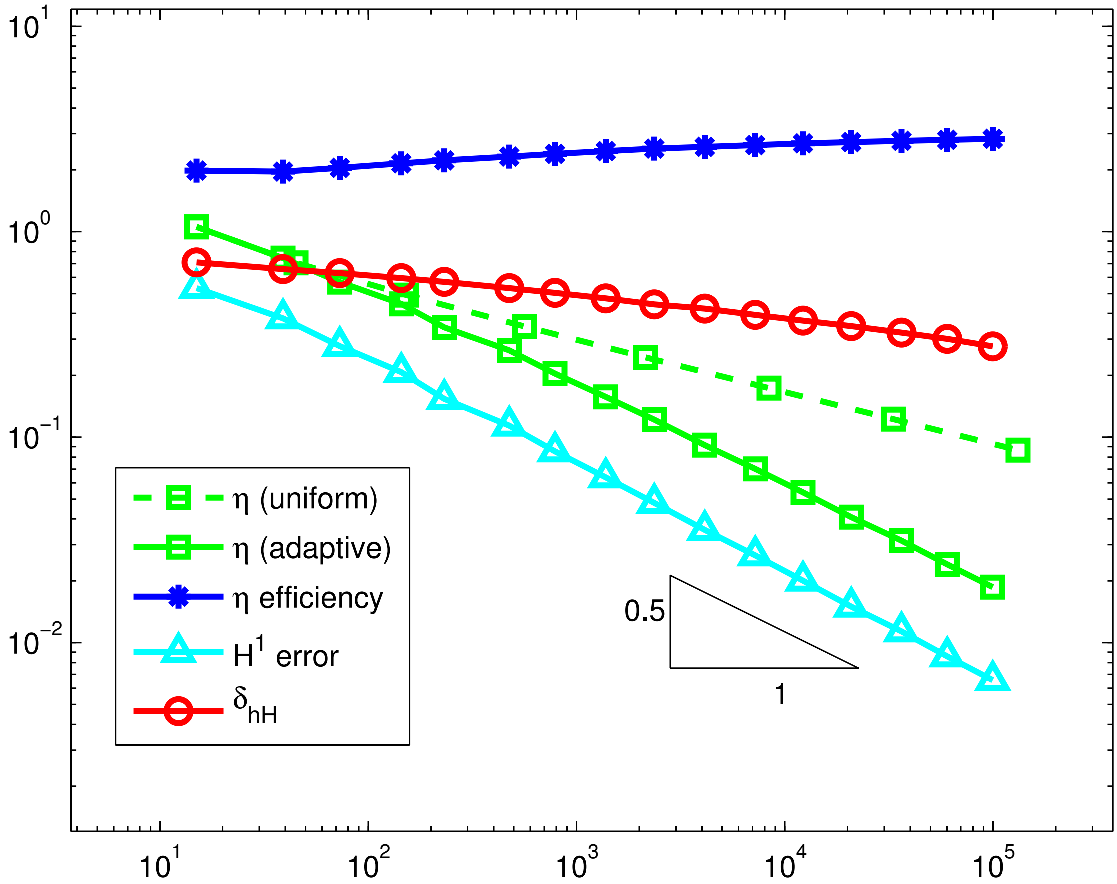

Figure 9: Estimator η, δ_{hH}, energy error and efficiency index for slit domain of Section 4.4 with singularity at the slit tip at $(0,0)$ for adaptive and uniform refinements.

As in the previous example, the solution exhibits a singularity at the crack tip. Again, the convergence rate is reduced in the case of uniform refinement and it can be recovered with an adaptive refinement based on the hierarchical error estimator. Moreover, when examining δ_{hH} in Figure 9, it becomes clear that the higher order solution on the coarser mesh only can provide the required order if an adaptive algorithm is chosen.

An adaptively refined mesh based on the hierarchical error estimator is shown in Figure 7 (right). As before, the refinement is concentrated around the singularity at the slit tip at the origin.

4.5 Overall conclusions

Some concluding remarks summarise the observations gathered from the numerical experiments.

(a) The error estimator η_h behaves reliably in all benchmarks although the higher-order approximation term is neglected. This follows from the convergence history plots where δ_{hH} is significantly smaller than one. The latter is observed for the coarsest mesh while even $\delta_{hH} \to 0$ as the level $\ell \to \infty$.

(b) The weighted error estimator $\eta_h/\sqrt{1-q^2}$ exhibits an efficiency index between 2 and 4.

(c) In all numerical examples, the adaptive algorithm performs better than uniform refinement and is able to recover an even optimal convergence rate.

References

[AAA04] B. Achchab, S. Achchab, and A. Agouzal, *Some remarks about the hierarchical a posteriori error estimate*, Numer. Methods Partial Differential Equations **20** (2004), no. 6, 919–932. MR 2092413 (2005k:65225)

[Ago02] Abdellatif Agouzal, *On the saturation assumption and hierarchical a posteriori error estimator*, Comput. Methods Appl. Math. **2** (2002), no. 2, 125–131. MR 1930842 (2003j:65111)

[AO00] Mark Ainsworth and J. Tinsley Oden, *A posteriori error estimation in finite element analysis*, Pure and Applied Mathematics (New York), Wiley-Interscience [John Wiley & Sons], New York, 2000. MR 1885308 (2003b:65001)

[BC02] Sören Bartels and Carsten Carstensen, *Each averaging technique yields reliable a posteriori error control in FEM on unstructured grids. II. Higher order FEM*, Math. Comp. **71** (2002), no. 239, 971–994 (electronic). MR 1898742 (2003e:65207)

[BCD04] Sören Bartels, Carsten Carstensen, and Georg Dolzmann, *Inhomogeneous Dirichlet conditions in a priori and a posteriori finite element error analysis*, Numer. Math. **99** (2004), no. 1, 1–24. MR 2101782 (2005i:65166)

[BEK96] Folkmar A. Bornemann, Bodo Erdmann, and Ralf Kornhuber, *A posteriori error estimates for elliptic problems in two and three space dimensions*, SIAM J. Numer. Anal. **33** (1996), no. 3, 1188–1204. MR 1393909 (98a:65161)

[BR01] Roland Becker and Rolf Rannacher, *An optimal control approach to a posteriori error estimation in finite element methods*, Acta Numer. **10** (2001), 1–102. MR 2009692 (2004g:65147)

[BR03] Wolfgang Bangerth and Rolf Rannacher, *Adaptive finite element methods for differential equations*, Lectures in Mathematics ETH Zürich, Birkhäuser Verlag, Basel, 2003. MR 1960405 (2004b:65002)

[Bra07] Dietrich Braess, *Finite elements*, third ed., Cambridge University Press, Cambridge, 2007, Theory, fast solvers, and applications in elasticity theory, Translated from the German by Larry L. Schumaker. MR 2322235 (2008b:65142)

[BS93] Randolph E. Bank and R. Kent Smith, *A posteriori error estimates based on hierarchical bases*, SIAM J. Numer. Anal. **30** (1993), no. 4, 921–935. MR 1231320 (95f:65212)

[BS08] Susanne C. Brenner and L. Ridgway Scott, *The mathematical theory of finite element methods*, third ed., Texts in Applied Mathematics, vol. 15, Springer, New York, 2008. MR 2373954 (2008m:65001)

[BW85] Randolph E. Bank and A. Weiser, *Some a posteriori error estimators for elliptic partial differential equations*, Math. Comp. **44** (1985), no. 170, 283–301. MR 777265 (86g:65207)

[Car99] Carsten Carstensen, *Quasi-interpolation and a posteriori error analysis in finite element methods*, M2AN Math. Model. Numer. Anal. **33** (1999), no. 6, 1187–1202. MR 1736895 (2001a:65135)

[Car04] ———, *Some remarks on the history and future of averaging techniques in a posteriori finite element error analysis*, ZAMM Z. Angew. Math. Mech. **84** (2004), no. 1, 3–21. MR 2031241 (2005d:65204)

[CB02] Carsten Carstensen and Sören Bartels, *Each averaging technique yields reliable a posteriori error control in FEM on unstructured grids. I. Low order conforming, nonconforming, and mixed FEM*, Math. Comp. **71** (2002), no. 239, 945–969 (electronic). MR 1898741 (2003e:65212)

[CBK01] Carsten Carstensen, Sören Bartels, and Roland Klose, *An experimental survey of a posteriori Courant finite element error control for the Poisson equation*, Adv. Comput. Math. **15** (2001), no. 1-4, 79–106 (2002), A posteriori error estimation and adaptive computational methods. MR 1887730 (2003a:65104)

[CF01] Carsten Carstensen and Stefan A. Funken, *Averaging technique for FE—a posteriori error control in elasticity. I. Conforming FEM, CMAME 190, 2483–2498., Averaging technique for FE—a posteriori error control in elasticity. II. λ-independent estimates, CMAME 190, 4663–4675., Averaging technique for a posteriori error control in elasticity. III. Locking-free nonconforming FEM, CMAME 191, 861–877.*

[CGG15] Carsten Carstensen, Dietmar Gallistl, and Joscha Gedicke, *Justification of the saturation assumption*, Numerische Mathematik (2015), available online.

[CGR12] Carsten Carstensen, Joscha Gedicke, and Donsub Rim, *Explicit error estimates for Courant, Crouzeix-Raviart and Raviart-Thomas finite element methods*, J. Comput. Math. **30** (2012), no. 4, 337–353.

[CP07] Carsten Carstensen and Dirk Praetorius, *Averaging techniques for a posteriori error control in finite element and boundary element analysis*, Boundary element analysis, Lect. Notes Appl. Comput. Mech., vol. 29, Springer, Berlin, 2007, pp. 29–59. MR 2298798 (2008b:65143)

[CV99] Carsten Carstensen and Rüdiger Verfürth, *Edge residuals dominate a posteriori error estimates for low order finite element methods*, SIAM J. Numer. Anal. **36** (1999), no. 5, 1571–1587 (electronic). MR 1706735 (2000g:65115)

[DN02] Willy Dörfler and Ricardo H. Nochetto, *Small data oscillation implies the saturation assumption*, Numer. Math. **91** (2002), no. 1, 1–12. MR 1896084 (2003e:65195)

[FLOP10] Samuel Ferraz-Leite, Christoph Ortner, and Dirk Praetorius, *Convergence of simple adaptive Galerkin schemes based on $h - h/2$ error estimators*, Numer. Math. **116** (2010), no. 2, 291–316. MR 2672266 (2011f:65257)

[Noc93] Ricardo H. Nochetto, *Removing the saturation assumption in a posteriori error analysis*, Istit. Lombardo Accad. Sci. Lett. Rend. A **127** (1993), no. 1, 67–82 (1994). MR 1284844 (95c:65187)

[Rod94] Rodolfo Rodríguez, *A posteriori error analysis in the finite element method*, Finite element methods (Jyväskylä, 1993), Lecture Notes in Pure and Appl. Math., vol. 164, Dekker, New York, 1994, pp. 389–397. MR 1300004 (95g:65158)

[Ver96] R. Verfürth, *A review of a posteriori error estimation and adaptive mesh-refinement techniques*, Wiley-Interscience [John Wiley & Sons], New York, 1996.

[ZZ87] O. C. Zienkiewicz and J. Z. Zhu, *A simple error estimator and adaptive procedure for practical engineering analysis*, Internat. J. Numer. Methods Engrg. **24** (1987), no. 2, 337–357. MR 875306 (87m:73055)